# Zinc−Thiolate Intermediate in Catalysis of Methyl Group Transfer in *Methanosarcina barkeri*†

Simonida Gencic,‡ Gilles M. LeClerc,‡,§ Natalia Gorlatova,‡,|| Katrina Peariso,⊥,# James E. Penner-Hahn,*,⊥ and David A. Grahame*,‡

*Department of Biochemistry and Molecular Biology, Uniformed Services University of the Health Sciences, 4301 Jones Bridge Road, Bethesda, Maryland 20814-4799, and Department of Chemistry, The University of Michigan, 930 North University Avenue, Ann Arbor, Michigan 48109-1055*

*Received June 20, 2001; Revised Manuscript Received August 21, 2001*

ABSTRACT: Methyl group transfer reactions are essential in methane-forming pathways in all methanogens. The involvement of zinc in catalysis of methyl group transfer was studied for the methyltransferase enzyme MT2-A important for methanogenesis in *Methanosarcina barkeri* growing on methylamines. Zinc was shown to be required for MT2-A activity and was tightly bound by the enzyme with an apparent stability constant of $10^{13.7}$ at pH 7.2. Oxidation was a factor influencing activity and metal stoichiometry of purified MT2-A preparations. Methods were developed to produce inactive apo MT2-A and to restore full activity with stoichiometric reincorporation of $Zn^{2+}$. Reconstitution with $Co^{2+}$ yielded an enzyme with 16-fold higher specific activity. Cysteine thiolate coordination in $Co^{2+}$−MT2-A was indicated by high absorptivity in the 300−400 nm charge transfer region, consistent with more than one thiolate ligand at the metal center. Approximate tetrahedral geometry was indicated by strong d−d transition absorbance centered at 622 nm. EXAFS analyses of $Zn^{2+}$−MT2-A revealed 2S + 2N/O coordination with evidence for involvement of histidine. Interaction with the substrate CoM (2-mercaptoethanesulfonic acid) resulted in replacement of the second N/O group with S, indicating direct coordination of the CoM thiolate. UV−visible spectroscopy of $Co^{2+}$−MT2-A in the presence of CoM also showed formation of an additional metal−thiolate bond. Binding of CoM over the range of pH 6.2−7.7 obeyed a model in which metal−thiolate formation occurs separately from $H^+$ release from the enzyme−substrate complex. Proton release to the solvent takes place from a group with apparent p$K_a$ of 6.4, and no evidence for metal−thiolate protonation was found. It was determined that substrate metal−thiolate bond formation occurs with a $\Delta G^{\circ\prime}$ of −6.7 kcal/mol and is a major thermodynamic driving force in the overall process of methyl group transfer.

The methanogenic Archaea employ a number of different methyl group transfer reactions in various pathways leading to methane formation. Methyl group transfer taking place at the penultimate step in methanogenesis utilizes coenzyme M[1] (2-mercaptoethanesulfonic acid) as the methyl group acceptor. The methyl group is donated by a corrinoid protein, which may be either a component of a membrane-bound, sodium ion translocating complex or a soluble corrinoid protein species, free or in association with one of a group of different methyltransferase enzymes. Several different corrinoid proteins have been identified recently which take part in the metabolism of different growth substrates in *Methanosarcina barkeri* (*1*−*5*). Substrates such as methanol and methylamines are acted on by specific methyltransferases (general designation methyltransferase 1, MT1) that bring about selective methylation of corrinoid proteins, as shown in reaction 1, in which X stands for −OH, $-NH_2$, $-NHCH_3$,

$$CH_3{-}X + [Co^{1+}]\text{corrinoid protein} + H^+ \xrightarrow{\text{MT1}} H{-}X + [CH_3{-}Co^{3+}]\text{corrinoid protein} \quad (1)$$

or $-N(CH_3)_2$. Transfer of the methyl moiety to the sulfhydryl group of coenzyme M is catalyzed by the enzyme methylcobamide:CoM methyltransferase (methyltransferase 2, MT2),

† This work was supported by grants from the National Science Foundation (MCB-9905068) and The U.S. Department of Energy (DE-FG02-00ER15108) (to D.A.G.) and the National Institutes of Health (GM38047) (to J.E.P.-H.).

* Correspondence should be addressed to these authors. D.A.G.: tel, 301-295-3555; fax, 301-295-3512; e-mail, dgrahame@usuhs.mil. J.E.P.-H.: tel, 734-764-7324; fax, 734-647-4865; e-mail, jeph@umich.edu.

‡ Uniformed Services University of the Health Sciences.

§ Present address: Department of Cell Biology, Medical University of South Carolina, Charleston, SC 29425.

|| Present address: American Red Cross, Rockville, MD 20855.

⊥ The University of Michigan.

# Present address: Department of Chemistry, University of New Mexico, Albuquerque, NM 87131.

[1] Abbreviations: Bis-Tris, bis(2-hydroxyethyl)iminotris(hydroxymethyl)methane; CDTA, *trans*-1,2-diaminocyclohexane-*N*,*N*,*N*′,*N*′-tetraacetic acid; coenzyme M, CoM, or HS-CoM, 2-mercaptoethanesulfonic acid; EXAFS, extended X-ray absorption fine structure; HEPES, *N*-(2-hydroxyethyl)piperazine-*N*′-2-ethanesulfonic acid; ICP-AES, inductively coupled plasma-atomic emission spectroscopy; MOPS, 3-(*N*-morpholino)propanesulfonic acid; MT2, methylcobamide:coenzyme M methyltransferase; MT2-A, MT2 isozyme A (also designated MtbA); MT2-M, MT2 isozyme M (or MtaA); TCEP, tris(2-carboxyethyl)phosphine hydrochloride; XANES, X-ray absorption near edge structure.

10.1021/bi0112917 CCC: $20.00 
Published on Web 10/03/2001

as shown in reaction 2. Two different isozymes of MT2

$$HS-CoM + [CH_3-Co^{3+}]\text{corrinoid protein} \xrightarrow{MT2} CH_3-S-CoM + [Co^{1+}]\text{corrinoid protein} + H^+ \quad (2)$$

[designated MT2-A and MT2-M (*6*)] interact with different corrinoid proteins in a highly selective fashion. Both isozymes are monomeric proteins with molecular masses of 36−37 kDa. The specificity of MT2/corrinoid protein−protein interactions is thought to explain why one isozyme, MT2-M, functions only in the metabolism of one substrate (methanol) whereas the other isozyme, MT2-A, is involved in conversion of several others (methylamines) (*7*).

Catalysis by MT2 proceeds by nucleophilic substitution, with attack of CoM on the methylcorrinoid $Co^{3+}$−methyl group and expulsion of the demethylated corrinoid in the $Co^{1+}$ form. Both MT2 isozymes contain zinc and are strongly inhibited by EDTA. A stoichiometry of 1 mol of Zn/mol of MT2 is probable, although some variability has been observed among different preparations (*8*). Direct involvement of Zn in catalysis by MT2 was first postulated (*8*) on the basis of analogy to the reaction of S-methylation of the zinc-bound Cys69 thiolate in the Ada DNA repair protein (*9*). In MT2 zinc would function similarly to "activate" CoM in the process of coordination by deprotonation of the thiol at neutral pH to generate a more nucleophilic thiolate species. Proton release upon addition of CoM to MT2-M at pH 7.7 has been demonstrated (*10*), consistent with the proposed role of the metal in deprotonation. However, direct evidence for thiolate coordination to zinc in MT2 has not yet been presented, and further insight is needed into the mechanism of methyl group transfer.

In the present study we provide evidence for direct binding of the substrate thiolate to the metal center in MT2-A by EXAFS analysis of the native protein and by UV−visible spectroscopy of a highly active, $Co^{2+}$-substituted form of the enzyme. The results unequivocally establish MT2-A as a member of a family of alkyltransferase enzymes in which zinc plays a direct role in catalysis, which include *Escherichia coli* methionine synthases (*11*) and rat protein farnesyltransferase (*12*). Additional insight into the mechanism of thiol activation was obtained by analysis of the thermodynamics of CoM binding to $Co^{2+}$−MT2-A over a range of pH. Evidence for a zinc−thiolate intermediate in methyltransferase catalysis is presented. Substrate metal−thiolate formation, as opposed to metal−thiol coordination, was found to predominate throughout the range of pH examined (pH 6.2−7.7). The results suggest that the mechanism of methyl group transfer involves metal−thiolate bond formation in a thermodynamically highly favorable reaction in which deprotonation of the substrate is achieved. This step is indicated to be the major driving force for the overall reaction. The issue of variation in Zn:MT2-A stoichiometry is also addressed, confirming a 1:1 molar ratio. The results are interpreted in the context of a zinc-mediated mechanism for thiol deprotonation in catalysis of methyl group transfer.

## MATERIALS AND METHODS

*Reagents*. All commercially available chemicals were obtained from Sigma Chemical Co., except as otherwise mentioned, and were of the highest purity grade offered. All solutions were prepared using Milli-Q deionized water (Millipore Corp.). All anaerobic procedures were performed using a Coy-type anaerobic chamber.

*MT2 Assay*. In vitro, MT2 is also capable of reacting with non-protein-bound corrinoid derivatives, and methylcobalamin was employed as a model methyl group donor substrate for routine measurements of enzymatic activity. The activity of MT2-A was measured spectrophotometrically by monitoring the conversion of methylcobalamin to cob(I)alamin at 25 °C in reaction mixtures containing 50 $\mu$M methylcobalamin, 100 $\mu$M coenzyme M, and 25 mM sodium 3-(*N*-morpholino)propanesulfonate (MOPS) buffer, pH 7.2, in dim light, under strictly anaerobic conditions. Reactions were initiated by addition of enzyme. All methylcobalamin solutions were standardized using the value of $\epsilon_{525nm} = 7.6\ mM^{-1}\ cm^{-1}$ (*13*). Because enzyme activity at levels of methylcobalamin below ≈1 mM is a nearly linear function of methylcobalamin concentration [$K_m$ for methylcobalamin = 14 mM (*8*)], all activity values have been normalized to conditions of 1 mM methylcobalamin. One unit of activity is defined as that amount of enzyme catalyzing methyl group transfer at 1 $\mu$mol/min at 25 °C under the normalized conditions.

*Overexpression and Purification of MT2-A*. MT2-A was overexpressed in *E. coli* using a modified pQE60 (QIAGEN) vector from which the 6×His tag had been deleted. A 1039 bp PCR fragment containing the coding sequence of MT2-A (GenBank accession number U38919) was obtained using *M. barkeri* strain NIH genomic DNA as template and a forward primer (5′-TTATCCATGGCAGAATATACCCCAAAAG-3′) with an integrated *Nco*I site and a reverse primer (5′-TTCAGGATCCTTTTTAGTATGTGTGGCTTTTTG-3′) containing a *Bam*HI site. The PCR product was blunt ended by treatment with T4 DNA polymerase (New England BioLabs) and after phosphorylation at the 5′ ends with T4 polynucleotide kinase (New England BioLabs) was subcloned into the *Sma*I site of pBluescript KS+ (Stratagene). The isolated plasmid was digested with *Nco*I and *Bam*HI, yielding a 1029 bp fragment which was purified by agarose gel electrophoresis and cloned into a modified pQE60 vector, designated pQE60m. The modification consisted of removal of the 6×His tag by digestion of pQE60 with *Hin*dIII and *Bgl*II, filling in with *E. coli* DNA polymerase I large fragment, Klenow (New England BioLabs), and religation of the blunt-ended vector. The *E. coli* strain M15[pREP4] was transformed with pQE60m carrying the MT2-A insert.

For purification of recombinant MT2-A *E. coli* was grown aerobically at 30 °C in Luria−Bertani (LB) medium supplemented with ampicillin (100 $\mu$g/mL) and kanamycin (25 $\mu$g/mL) to an $OD_{600nm}$ of 0.6, whereupon isopropyl $\beta$-D-thiogalactopyranoside (IPTG) and $ZnSO_4$ were added to final concentrations of 1 mM and 50 $\mu$M, respectively. Cells were harvested 6 h after induction. Cell paste (14.3 g) was resuspended in 26 mL of solution A (50 mM Tris·$H_2SO_4$, 25 mM $Na_2SO_4$, pH 7.5), and cells were lysed at 0−4 °C by French press disruption at 20 000 psi. The lysate was diluted by addition of 40 mL of ice-cold solution A and centrifuged at 2 °C for 25 min at 27000*g*. The supernatant was adjusted to a total volume of 100 mL with solution A and subjected to chromatography at room temperature on a column (10 × 5.0 cm diameter) of Q-Sepharose Fast Flow (Pharmacia) previously equilibrated in solution A. MT2-A was eluted

Table 1: Site-Directed Mutagenesis of MT2 Isozymes

| | specific activity (% of wild type)[b] | |
|---|---|---|
| mutant[a] | MT2-A | MT2-M |
| H47N | 78 | |
| C84S | 98 | |
| H239F | 0.0 | |
| H239N | 0.0 | 0.0 |
| H239C | 0.0 | |
| C241S | 0.4 | 0.1 |
| C316S | 0.0 | 0.0 |

[a] Amino acid residue numbering is based on the MT2-A sequence. [b] Wild-type extracts were from XL1-Blue MRF′ cells transformed with pMA83 and pMET82 expressing MT2-A and MT2-M wild-type isozymes, respectively.

isocratically with solution A and after adjustment to contain 50 mM bis(2-hydroxyethyl)iminotris(hydroxymethyl)methane (Bis-Tris) and 0.5 M $Na_2SO_4$, pH 6.6, was applied to a column (15.5 × 2.5 cm diameter) of phenyl-Sepharose (Pharmacia) equilibrated in solution B (50 mM Bis-Tris, 0.5 M $Na_2SO_4$, pH 6.5). The column was eluted with a 200 mL linear gradient of solution B decreasing from 100% to 0% versus 20 mM Bis-Tris, pH 6.5. The final preparation was obtained by concentrating the pooled fractions and diafiltration against 20 mM Bis-Tris, pH 6.5, on an Amicon stirred cell equipped with a YM-30 ultrafiltration membrane to a final volume of 30 mL containing MT2-A at a concentration of 16.5 mg/mL. Protein was determined on the basis of absorbance at 280 nm using an absorptivity coefficient for MT2-A of 0.9102 mg $mL^{-1}$ $cm^{-1}$, corresponding to 33 400 $M^{-1}$ $cm^{-1}$ which was obtained from the expression $1.03(5550\sum Trp + 1340\sum Tyr + 150\sum Cys)$, according to the method of Perkins (*14*).

Metal analyses were carried out by ICP-atomic emission spectroscopy using a Thermo Jarrell-Ash 965 AtomComp plasma emission spectrometer on samples submitted to the University of Georgia, Research Services, Chemical Analysis Laboratory.

*Site-Directed Mutagenesis of MT2-A and MT2-M*. Conserved cysteine and histidine residues are present at five separate sites in the MT2 isozymes. Site-directed mutagenesis was performed on three of these sites in MT2-M and on all five in MT2-A using the procedure of Kunkel (*15*). The *M. barkeri* genomic fragments containing the genes for MT2-A and MT2-M were subcloned into pBluescript II SK (+) and (−) phagemids for mutagenesis. The phagemids pMA85 and pMA83 with a 4.5 kb *Eco*RI insert carrying the gene for MT2-A and pMET84 and pMET82 containing the gene for MT2-M on a 3.6 kb *Hin*dIII insert were employed for mutagenesis of MT2-A and MT2-M, respectively. These phagemid DNAs were used to transform *E. coli* $dut^-$ $ung^-$ strain CJ236. Following infection with helper phage M13K07, single-stranded, uracil-containing DNA was isolated and annealed with 16−29mer, 5′-phosphorylated mutagenic primers designed to produce the single-site substitutions indicated in Table 1. After reaction with DNA polymerase and ligation the double-stranded, closed circular DNA containing uracil on the parental strand was used to transform $ung^+$ *E. coli* XL1-Blue MRF′. Each mutant genotype was confirmed by sequencing isolated plasmid DNA in the region containing the mutation site with Sequenase Version 2.0 (Amersham Pharmacia). The activity of MT2 mutants was quantified after an initial screen which was based on visual inspection of the red to brown color change accompanying demethylation of methylcobalamin in modified assay mixtures. Cells collected from 1 mL overnight cultures were resuspended in 75 μL of Tris buffer, pH 7.5, containing 2.5 μg/mL lysozyme and 2% Tween 20, and samples of the resulting lysates (40 μL) were used in 500 μL assays carried out at room temperature in 24-well microtiter plates protected from light. For mutants displaying activity the color change was observable within minutes, whereas inactive mutants and control samples lacking MT2 gene inserts showed no noticeable change even after overnight incubation. In all cases, expression of full-length mutant proteins was verified by Western blot analyses using polyclonal antibodies specific for the different MT2 isozymes (*6*).

*Effect of $Zn^{2+}$ and $Co^{2+}$ on the Activity of MT2-A.* Purified MT2-A was incubated at a concentration of 3.30 mg/mL under anaerobic conditions overnight at 25 °C in 50 mM sodium *N*-(2-hydroxyethyl)piperazine-*N*′-2-ethanesulfonate (HEPES) buffer, pH 7.2, in the absence or presence of 1 mM EDTA. Samples were then diluted under anaerobic conditions in 50 mM HEPES, pH 7.2, to 0.66 mg/mL (one-fifth dilution) in the presence or absence of $ZnSO_4$ or $CoCl_2$ such that the final total metal ion concentration was 100 μM in excess of the final concentration of EDTA. After incubation for 10 min at 25 °C samples were withdrawn and assayed for activity as described in the previous section. In experiments to test the effect of reducing agent, tris(2-carboxyethyl)phosphine hydrochloride (TCEP, Calbiochem) was also added during the dilution to give a final concentration of 1 mM. The effect of $H_2O_2$ on the EDTA-treated enzyme was tested separately by including 0.1 mM $H_2O_2$ during the overnight incubation with EDTA. Control experiments in which higher concentrations of metals were present and/or longer times of incubation were used did not result in higher levels of activity. The level of metal ion contamination in solutions was monitored by ICP analysis and did not affect the final activity values. However, in preliminary assays employing high concentrations of CoM (2 mM) and methylcobalamin (1 mM), partial reactivation of apo MT2-A was observed, attributable to trace metal ion contamination of the assay mixtures found by ICP analysis of stock solutions to originate from the large amounts of substrates used.

*EXAFS Sample Preparation, Data Collection, and Analysis.* Purified MT2-A was concentrated by ultrafiltration using prewashed Centricon 30 (Amicon-Millipore) devices at 8 °C maintained under anaerobic conditions. Samples were then adjusted to contain approximately 27% glycerol at a final concentration of Zn−MT2-A between 3.0 and 3.4 mM. Coenzyme M, when present, was added at a 3-fold molar excess. Samples were loaded into Lucite cuvettes (≈150 μL) with 40 μm Kapton tape windows and frozen rapidly in liquid nitrogen.

Zinc XAS data were recorded for three independently prepared samples of MT2-A and two independently prepared samples of MT2-A + CoM. Measurements were made at the Stanford Synchrotron Radiation Laboratory (SSRL) on beamline 9-3, using a fully tuned Si(220) double-crystal monochromator with a Rh-coated upstream mirror for harmonic rejection. Data collection and calibration were as previously described (*16*, *17*), utilizing a 30-element Ge

solid-state detector array. The total incident count rates were held below 105 kHz per channel to avoid saturation, and the windowed Zn Kα count rates were 17−42 kHz per channel in the EXAFS region, giving (8.5−21) × $10^6$ usable counts per scan at $k = 13$ Å$^{-1}$. Each channel was examined for glitches, and the good channels were averaged (24−26 channels per scan) to give the final EXAFS spectrum, with four or five scans averaged per spectrum.

X-ray absorption near edge structure (XANES) data normalization and the EXAFS data reduction followed procedures described previously (*16*). Fourier transforms were calculated using $k^3$-weighted data over a range of 2−12.8 Å$^{-1}$ for MT2-A sample 1, 2−11.8 Å$^{-1}$ for sample 2, and 2−12.4 Å$^{-1}$ for sample 3 and both samples containing CoM. The first shell ($R + \alpha = 0.8-3.0$ Å) was then back-transformed over the same range. Fits to both the filtered and unfiltered data were performed as described previously (*18*), using the program Feff v.6.0.1 (*19*, *20*) to calculate the theoretical phase and amplitude functions for a Zn−N at 2.05 Å and a Zn−S at 2.35 Å. Filtered and unfiltered data gave equivalent structural parameters.

*$Co^{2+}$ Reconstitution of Apo MT2-A*. Apo MT2-A was prepared by anaerobic overnight incubation of MT2-A (4.13 mg/mL) at 25 °C with 10 mM *trans*-1,2-diaminocyclohexane-*N*,*N*,*N*′,*N*′-tetraacetic acid (CDTA) in 50 mM HEPES, pH 7.2, followed by anaerobic gel filtration to remove CDTA and complexed metal ion. Gel filtration of 800 μL samples of the CDTA-treated MT2-A was carried out on a 1.5 cm diameter, 18 mL column of Sephadex G-50 (Pharmacia) equilibrated with 25 mM HEPES, pH 7.2, previously treated with CDTA and washed to remove trace metal ions. Fractions containing apo MT2-A free of CDTA were combined and concentrated under anaerobic conditions to a volume of approximately 200 μL using a prewashed Centricon 30 (Amicon-Millipore) centrifugal ultrafiltration device. The concentrate was then brought to a final volume of 625 μL with 25 mM HEPES, pH 7.2, and adjusted to contain 1 mM TCEP in a 1.5 mL semi-micro spectrophotometer cuvette. After incubation for 20−40 min $Co^{2+}$ reconstitution of the enzyme was initiated by anaerobic titration with $CoCl_2$. UV−visible spectra were recorded in the absence of $Co^{2+}$ and after each consecutive 5 μL addition of a stock solution of 2.5 mM $CoCl_2$ in 1 mM $H_2SO_4$. After reaching equivalence, the blue enzyme was removed from the cuvette and applied to a 1.5 cm diameter, 10 mL column of Sephadex G-25 (Pharmacia) equilibrated with 25 mM HEPES, pH 7.2, to remove excess $Co^{2+}$. Fractions were collected, combined, and concentrated under anaerobic conditions as before.

*Coenzyme M Binding to MT2-A Reconstituted with $Co^{2+}$*. Binding of coenzyme M to the $Co^{2+}$-substituted enzyme was monitored spectrophotometrically under anaerobic conditions. Separate samples of $Co^{2+}$−MT2-A in the range of 175−230 μM were prepared at different pH values by carrying out the Sephadex G-25 step for excess $Co^{2+}$ removal using buffers of different pH values; 25 mM HEPES was used for samples prepared above pH 7, whereas 25 mM Bis-Tris was employed for experiments below pH 7.0. Concentrated fractions from G-25 chromatography at the indicated pH were transferred to a semi-micro spectrophotometer cuvette and made up to 590 μL by addition of the same column buffer. Titration was performed by addition of aliquots (2.5, 5.0, and in some cases 10 μL) of an 8.0 mM stock solution of coenzyme M. The absorbance ($A_{668nm} - A_{622nm}$) was related to the concentration of bound CoM, [ES], by the formula $[ES] = z[(A_{668nm} - A_{622nm}) - A_0]$, where $A_0$ is the value of ($A_{668nm} - A_{622nm}$) in the absence of CoM and $z$ is a proportionality factor. The absorbance was fitted as a function of total CoM concentration, $[S]_t$, to the quadratic binding equation according to Segel (*21*)

$$[ES] = \frac{[E]_t + [S]_t + K_d(obs) - \sqrt{([E]_t + [S]_t + K_d(obs))^2 - 4[E]_t[S]_t}}{2} \quad (3)$$

in which $[E]_t$ represents the total enzyme concentration, and $K_d$(obs) is the observed dissociation constant for the enzyme−CoM complex, using the program SigmaPlot (Jandel Corp.). The total CoM concentration $[S]_t$ is calculated in compliance with the increase in total volume that results from aliquot additions. However, because a slight decrease in $[E]_t$ also occurs after each aliquot is added, in the fit $[E]_t$ is allowed to decrease according to the formula $[E]_t = [E]_{total}/df$, where df values are the dilution factors resulting from aliquot additions. The resulting fits give values for $A_0$, $z$, $[E]_t$, and $K_d$(obs).

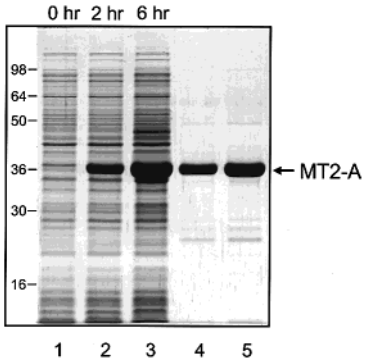


FIGURE 1: SDS−PAGE of overexpressed and purified MT2-A. Samples from the culture of *E. coli* strain M15[pREP4] transformed with pQE60m carrying the MT2-A insert were taken at the times indicated before and after induction with IPTG and analyzed on a 12% acrylamide/Tris−glycine/SDS gel stained with Coomassie blue R-250 (lanes 1−3). Lanes 4 and 5 contained the final MT2-A preparation, 3 and 6 μg, respectively. Positions of standard proteins are indicated with molecular mass values in kDa (SeeBlue prestained standard, Novex-Invitrogen).

## RESULTS

*Factors Influencing the Activity and Metal Content of Purified MT2-A*. Purification of MT2-A expressed in *E. coli* yielded preparations of approximately 98% purity as judged by densitometric analyses of SDS gels (Figure 1). Metal analysis by ICP-AES revealed 0.63 ± 0.03 ($n = 2$) mol of Zn/mol of MT2-A. This suggested the possibility of incomplete incorporation of metal. To determine whether the enzyme was capable of incorporating additional $Zn^{2+}$, the purified enzyme was incubated with 100 μM $ZnCl_2$. As shown in Figure 2 (top) 10 min exposure to $Zn^{2+}$ alone did not result in a significant increase in methyltransferase specific activity. Longer periods of incubation also had no effect. In contrast, addition of the reducing agent TCEP along with $Zn^{2+}$ increased the activity from around 43 to 56 units/mg. An even more pronounced effect was observed in

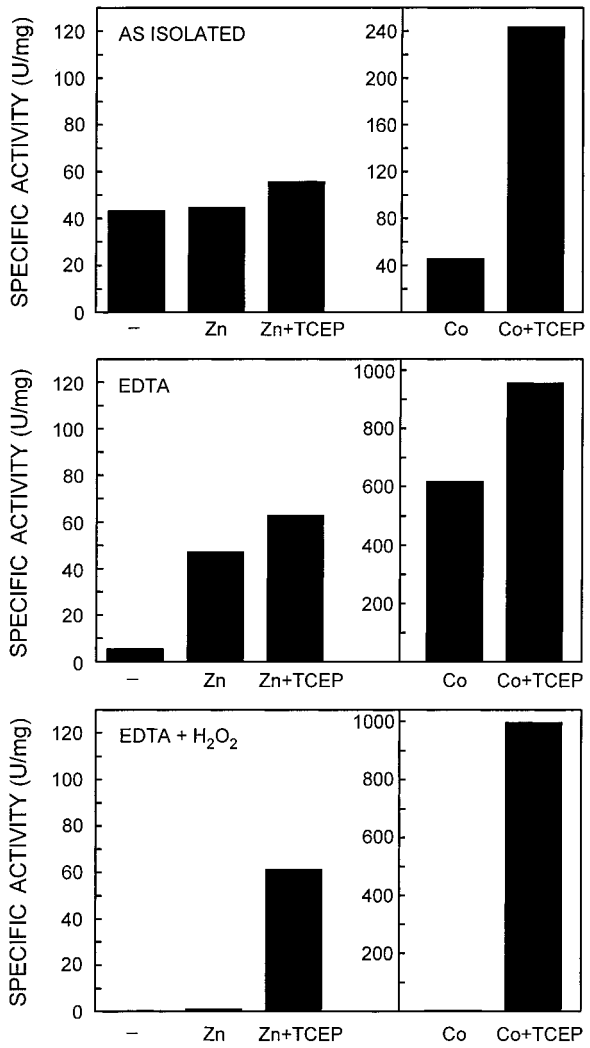


FIGURE 2: Effect of $Zn^{2+}$ and $Co^{2+}$ on the activity of native and EDTA-treated MT2-A in the presence and absence of reducing agent. Purified MT2-A was incubated overnight under anaerobic conditions in the absence (as isolated) or presence of 1 mM EDTA (EDTA) or in the presence of 1 mM EDTA plus 0.1 mM $H_2O_2$ (EDTA + $H_2O_2$), as described under Materials and Methods. The incubation mixtures were then diluted under different conditions prior to assay of methyltransferase activity. Dilutions were carried out with 50 mM HEPES, pH 7.2, in the absence of metals (−) or in the presence of 100 $\mu$M $Zn^{2+}$ or $Co^{2+}$. When EDTA was present, total concentrations of $Zn^{2+}$ and $Co^{2+}$ were 100 $\mu$M in excess over the final [EDTA]. The effect of exposure to metal ions and a reducing agent was examined by addition of 1 mM TCEP to the diluted enzyme samples (Zn + TCEP and Co + TCEP). The influence of oxidation on the EDTA-treated enzyme was tested by including 0.1 mM $H_2O_2$ during the overnight incubation (EDTA + $H_2O_2$).

incubations with $Co^{2+}$. By itself 100 $\mu$M $Co^{2+}$ had no noticeable effect, but combination with 1 mM TCEP provided a 5.5-fold elevation of specific activity (Figure 2, top). One possible explanation for the marked increase in activity would be that the enzyme was reduced by TCEP to a form capable of incorporating additional metal, with $Co^{2+}$−MT2-A possessing intrinsically higher specific activity than $Zn^{2+}$−MT2-A. To test this, the enzyme was first treated with a chelator to remove metal ions prior to the incubations. Treatment with 1 mM EDTA caused a marked loss of activity, and as shown in Figure 2 (middle), subsequent incubation with $Zn^{2+}$ restored activity to a level equal to or slightly greater than the original. Addition of TCEP again caused significant stimulation of activity. Moreover, addition of $Co^{2+}$ alone now afforded very high levels of activity, approximately 600 units/mg, which could be further stimulated by TCEP about 1.6-fold. These results are consistent with the idea that a portion of the enzyme which is incapable of binding metal exists in an oxidized form that can be reversibly reduced to a state competent to bind metal. Indeed, oxidation with 0.1 mM $H_2O_2$ yielded a form that was no longer able to be reactivated by simple addition of either $Zn^{2+}$ or $Co^{2+}$, as shown in Figure 2 (bottom). Nonetheless, full activity was regained in the presence of TCEP. Reversible disulfide formation from cysteine residues normally involved in metal ion coordination is one possibility consistent with these results, and candidates C241 and C316 are implicated, being essential for activity in site-directed mutagenesis experiments (Table 1).

Direct evidence for incorporation of additional $Zn^{2+}$ under reducing conditions is shown in Figure 3. Gel filtration was employed to monitor changes in the metal content of MT2-A following treatment with EDTA or after exposure to $Zn^{2+}$ in the presence of a reducing agent. Treated samples of the purified enzyme were subjected to gel filtration, and fractions were analyzed for metal content by ICP-AES. The zinc content of the enzyme obtained after treatment with $Zn^{2+}$ and TCEP was substantially higher (approximately 1.6 times) than in untreated samples (Figure 3). Overnight incubation with 2 mM EDTA removed nearly all of the zinc from the enzyme; however, a small amount associated with the protein was still detectable (Figure 3, bottom). Changes in the zinc content paralleled the changes in activity observed previously under similar conditions. It was concluded that a portion of the enzyme existed in an oxidized form lacking metal and that this was responsible for less than integer stoichiometry. The results indicated that a reduced form of the enzyme is required for metal binding to occur. Incorporation of $Co^{2+}$ by the reduced enzyme was suggested (later confirmed by $Co^{2+}$ reconstitution experiments; see below), and the $Co^{2+}$-containing enzyme exhibited approximately 16 times higher specific activity than the native $Zn^{2+}$-containing protein.

To examine direct involvement of the metal ion in methyl group transfer catalysis and to investigate the coordination environment in the protein, $Co^{2+}$ reconstitution experiments and Zn EXAFS analyses were performed.

*EXAFS Analysis of MT2-A.* Zinc XANES spectra and the Fourier transforms of the EXAFS data for MT2-A in the presence and absence of coenzyme M are shown in Figure 4. The XANES spectrum of the native enzyme showed two distinctive features of similar intensity at ≈9664 and ≈9669 eV that are very similar to those found in spectra of $ZnS_2N_2$ model complexes (*18*). Addition of the substrate CoM caused the spectrum to shift to lower energy, and the feature at ≈9664 eV showed a slight decrease in intensity while there was a more pronounced decrease in the intensity of the feature at 9669 eV. These changes are reminiscent of those found in the spectra of both cobalamin-dependent and cobalamin-independent methionine synthases from *E. coli* when the substrate homocysteine is added to these enzymes (*16*, *17*).

The structural origins of the XANES changes are clearly shown in the Fourier transforms (Figure 4) and fits to the EXAFS data (Table 2). The Fourier transform of the native

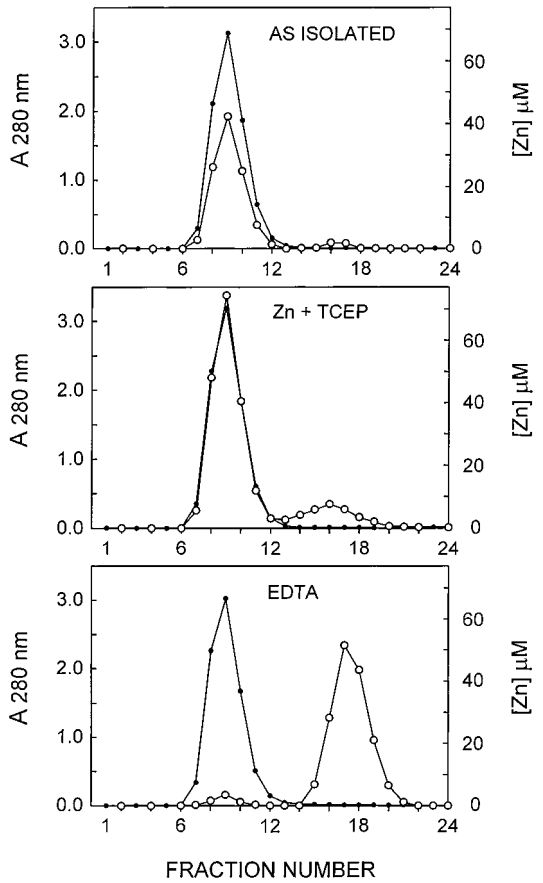


FIGURE 3: Changes in the zinc content of MT2-A following incubation with $Zn^{2+}$ and a reducing agent and after treatment with EDTA. Zinc content was measured after gel filtration of samples of MT2-A on an 18 mL column (1.5 cm diameter) of Sephadex G-50 in 25 mM HEPES, pH 7.2. Three samples were prepared for analysis; each contained 9.9 mg of MT2-A in 50 mM HEPES, pH 7.2, in a final volume of 1.2 mL. The sample designated "as isolated" contained no further additives. The sample designated Zn + TCEP contained in addition 200 $\mu$M $ZnSO_4$ and 1 mM TCEP and was incubated for approximately 1 h before application onto the column. The third sample, EDTA, contained 2 mM EDTA and was incubated overnight before chromatography. One milliliter fractions were collected, from which aliquots, 0.1 mL, were removed and diluted one-sixth for measurement of absorbance, shown plotted after correction for dilution (●). ICP metal analysis was carried out on the remaining portion of each fraction to obtain the concentration of zinc, as indicated (○). The column was made metal-free prior to each experiment by washing with EDTA and reequilibration in 25 mM HEPES buffer. All steps were performed under anaerobic conditions.

MT2-A EXAFS data has a single peak centered at $R + \alpha \approx 1.8$ Å with a broad low-$R$ shoulder, similar to the Fourier transforms of EXAFS data for $ZnS_2N_2$ models (*18*). Fits to the EXAFS data confirmed that the native MT2-A zinc site is best modeled as 2S at 2.30 Å and 2(N/O) ligands at 2.04 Å. Low-amplitude outer-shell scattering was also found for $R + \alpha \approx 2.3-3.9$ Å. These peaks compare well with those observed in zinc−tetraimidazole model complexes, and the amplitude of the outer-shell scattering in MT2-A suggests that at least one of the protein ligands to the zinc is a histidine residue. A candidate is H239, which along with C241 and C316 was found to be required for activity in site-directed mutagenesis experiments (Table 1).

After addition of CoM to a solution of the native MT2-A, the main peak in the Fourier transform shifted slightly to higher distance, the amplitude of the main peak increased, and the amplitude of the low-$R$ shoulder decreased. These observations are consistent with the replacement of a low-$Z$ (N/O) ligand with a higher-$Z$ ligand (e.g., S) upon binding of CoM. Fits to the MT2-A + CoM EXAFS data showed that the zinc site remains four-coordinate upon CoM binding, but it was best modeled as having 3S with a greater average bond distance of 2.33 Å and 1N or 1O ligand, also at greater average distance. These data suggest that the sulfur atom of the CoM thiol binds directly to the Zn in MT2-A.

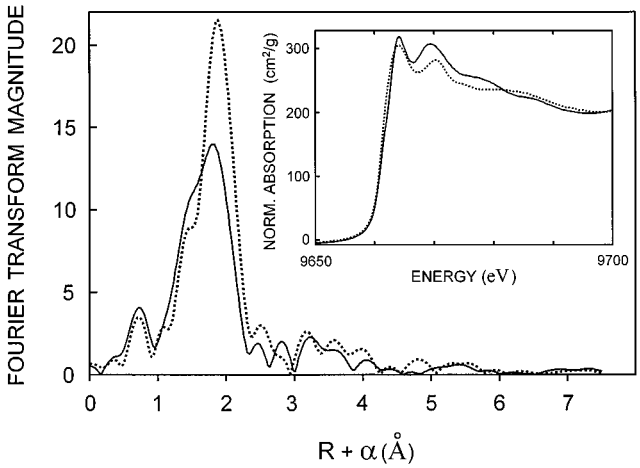


FIGURE 4: X-ray absorption spectroscopy of MT2-A. Fourier transforms of the zinc EXAFS data and normalized XANES spectra (inset) are shown for MT2-A (−) and MT2-A + CoM (- - -).

Table 2: Zinc Coordination Parameters of MT2-A ± CoM from EXAFS Fitting Analyses[a]

| | CN | $R_{ab}$ (Å) | $\sigma^2 \times 10^3$ (Å$^2$) | CN | $R_{ab}$ (Å) | $\sigma^2 \times 10^3$ (Å$^2$) | $F'$ |
|---|---|---|---|---|---|---|---|
| MT2-A | 4S | 2.284 | 6.9 | | | | 0.052 |
| (sample 1) | 3S | 2.291 | 4.5 | 1N | 2.025 | 1.4 | 0.031 |
| | **2S** | **2.296** | **2.3** | **2N** | **2.040** | **2.9** | **0.022** |
| MT2-A | 4S | 2.281 | 7.6 | | | | 0.056 |
| (sample 2) | 3S | 2.289 | 5.3 | 1N | 2.032 | 2.3 | 0.035 |
| | **2S** | **2.295** | **2.6** | **2N** | **2.037** | **3.3** | **0.020** |
| MT2-A | 4S | 2.29 | 8.3 | | | | 0.042 |
| (sample 3) | 3S | 2.30 | 5.6 | 1N | 2.02 | 1.5 | 0.026 |
| | **2S** | **2.30** | **3.0** | **2N** | **2.04** | **3.1** | **0.017** |
| MT2-A + CoM | 4S | 2.322 | 4.7 | | | | 0.027 |
| (sample 1) | **3S** | **2.327** | **2.6** | **1N** | **2.057** | **2.1** | **0.015** |
| | 2S | 2.332 | 0.4 | 2N | 2.078 | 2.6 | 0.023 |
| MT2-A + CoM | 4S | 2.32 | 5.0 | | | | 0.024 |
| (sample 2) | **3S** | **2.33** | **3.0** | **1N** | **2.07** | **2.8** | **0.014** |
| | 2S | 2.33 | 0.7 | 2N | 2.08 | 3.0 | 0.020 |

[a] Abbreviations: CN, coordination number and ligand type; $R_{ab}$, average bond distance; $\sigma^2$, mean squared deviation in $R_{ab}$ (Debye−Waller factor); $F'$, fitting error statistic. The best fits are shown in bold.

Further evidence for direct metal−sulfur ligation in the MT2-A·CoM complex was provided from experiments using UV−visible spectroscopy to analyze the effect of CoM on the $Co^{2+}$-substituted enzyme.

*Cobalt Reconstitution of Apo MT2-A.* A procedure for incorporation of $Co^{2+}$ into MT2-A was developed in which $Zn^{2+}$ was first removed from the enzyme by use of a chelator. Experiments with EDTA showed that significant residual levels of Zn and activity remained even at relatively high concentrations of the chelator. The ratio of inactive to active enzyme was calculated on the basis of activity measured after overnight incubation of several samples of 0.05 mM MT2-A

at pH 7.2 with total [EDTA] in the range of 0.2−2.0 mM. The results followed the equilibrium described by eq 4 and

$$\text{Zn}-\text{MT2}_{\text{active}} + \text{EDTA} \rightleftharpoons \text{MT2}_{\text{inactive}} + \text{Zn}-\text{EDTA} \quad (4)$$

yielded a value for the equilibrium constant of $K_{eq} = 0.36$. Using a value for the Zn−EDTA stability constant of $10^{13.3}$ at pH 7.2 [$K_1 = 10^{16.4}$ (*22*)], an affinity constant of $10^{13.7}$ was calculated for $Zn^{2+}$ binding to MT2-A. The results indicated that EDTA treatment would be inefficient for complete removal of Zn from the enzyme; therefore, a stronger chelator CDTA [$K_1 = 10^{19.1}$ (*22*)] was employed. At similar concentrations to EDTA, treatment with CDTA resulted in markedly lower levels of residual activity, consistent with the higher metal ion affinity of this chelator; however, the observed rate of inactivation with CDTA was significantly lower than with EDTA. For this reason 10 mM CDTA was employed in overnight incubations to generate apo MT2-A. Following removal of CDTA by gel filtration on a metal-free column of Sephadex G-50, apo MT2-A was titrated with $CoCl_2$. The titration was monitored spectrophotometrically with formation of a blue $Co^{2+}$−MT2-A complex clearly visible. Spectra obtained during $CoCl_2$ titration are shown in Figure 5A. Strong absorbance was observed in the 300−400 nm region, with a maximum absorptivity at 314 nm of 3000 $M^{-1}$ $cm^{-1}$. Absorbance in the 600 nm region was also evident with a major peak at 622 nm with an absorptivity of about 700 $M^{-1}$ $cm^{-1}$ flanked by minor peaks at 572 and 712 nm. Overall, the spectral characteristics were consistent with $Co^{2+}$ in tetrahedral coordination exhibiting d−d transitions in the region around 600 nm and with absorbance in the 300−400 nm region due to the $Co^{2+}$−thiolate charge transfer interaction. The end point of the titration was found by plotting the absorbance ($A_{622nm} - A_{572nm}$) versus the amount of $CoCl_2$ added. As shown in Figure 5B, absorbance was a linear function of the amount of $Co^{2+}$ added up to the end point. Typical values of the [$Co^{2+}$]/[MT2-A] ratio found at equivalence were in the range of 0.90−0.93. The results indicate a metal to MT2-A stoichiometry of 1:1. These titrations were carried out in the presence of 1 mM TCEP; however, it is noteworthy that in the absence of reducing agent the end point is reached at significantly lower amounts of $Co^{2+}$. The effect of TCEP on the titration was to increase $Co^{2+}$ incorporation by a factor of 1.5, a result consistent with the earlier finding that a portion of the enzyme as isolated exists in an inactive, oxidized state, which can bind metal only after reduction.

*Metal Thiolate Formation in Binding of CoM to MT2-A.* The $Co^{2+}$-reconstituted MT2-A, freed of excess $CoCl_2$ by gel filtration, was used in experiments to determine binding of the substrate CoM by UV−visible spectroscopy. As shown in Figure 6A, titration of the enzyme with CoM resulted in transformation of the spectrum of the $Co^{2+}$ enzyme in the ligand field region from the three peaks originally at 572, 622, and 712 nm to a new form with peaks at 616, 668, and 700 nm. Changes also occurred at lower wavelengths with increase in absorbance noted throughout the 300−400 nm region. Difference spectra in this region, shown in Figure 7, indicated the appearance of a prominent new band centered at 354 nm with an absorptivity of 1150 $M^{-1}$ $cm^{-1}$. Addition of other thiol-containing compounds at similar concentrations to CoM, such as L-cysteine, DL-homocysteine, 3-mercaptopropanesulfonic acid, and dithiothreitol, which are not substrates, and 3-mercaptopropionic acid, a weak substrate with an apparent $K_m$ roughly 500 times greater than CoM, had almost no effect on the spectrum of the $Co^{2+}$ enzyme. (At higher concentrations all of these compounds did exhibit slight interaction; however, their effects were $^1/_{500}$th to $^1/_{2000}$-th that of CoM.) The results indicated that upon binding of CoM an additional thiolate ligand is introduced into the $Co^{2+}$ coordination sphere and that tetrahedral geometry of the metal center is preserved. This agrees with the findings from EXAFS analysis of the zinc enzyme. Furthermore, the extent of absorptivity change in the charge transfer region was also consistent with the results from EXAFS, indicating a shift from 2-sulfur ligation in the native enzyme to 3-sulfur ligation in the presence of CoM. The absorbance ($A_{668nm} - A_{622nm}$) recorded during the titration was plotted as function

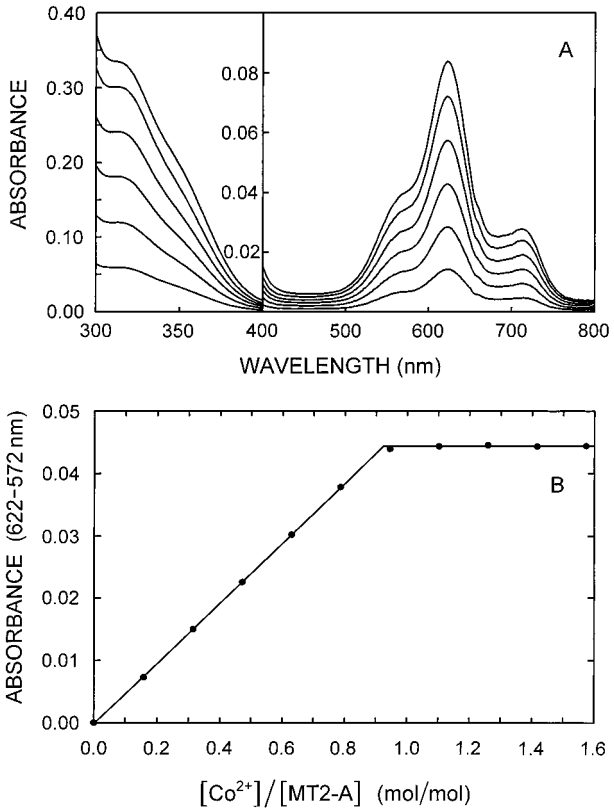


FIGURE 5: $Co^{2+}$ reconstitution of MT2-A. Incorporation of $Co^{2+}$ into apo MT2-A was monitored spectrophotometrically. Apo MT2-A was prepared by incubation with the chelator CDTA and subsequently isolated by gel filtration on Sephadex G-50 and concentrated. All procedures were carried out under anaerobic conditions, as described under Materials and Methods, and spectra were recorded on a Hewlett-Packard 8452A diode array spectrophotometer set up inside a Coy-type anaerobic chamber (*23*). Shown in panel A are the spectra recorded after sequential addition of 12.5, 25, 37.5, 50, 62.5, and 75 nmol of $CoCl_2$ to a solution (625 $\mu$L) containing 79.4 nmol of apo MT2-A, 1 mM TCEP, and 25 mM HEPES, pH 7.16. The spectra have been corrected for dilution due to aliquot additions by multiplying by the appropriate dilution factor, up to a maximum of 1.08. The absorbance scale at the left between 300 and 400 nm has been increased to show changes taking place in the $Co^{2+}$ ← S charge transfer region. The right side shows absorbance due to $Co^{2+}$ ligand field d−d transitions characteristic of the CoM·$Co^{2+}$−MT2-A complex. Panel B shows the absorbance ($A_{622nm}-A_{572nm}$) plotted as a function of the molar ratio of $Co^{2+}$ to MT2-A, with equivalence at 0.923 mol of $Co^{2+}$/mol of MT2-A. A molar absorptivity of $\epsilon_{622-572nm} = 379$ $M^{-1}$ $cm^{-1}$ was calculated on the basis of cobalt concentration.

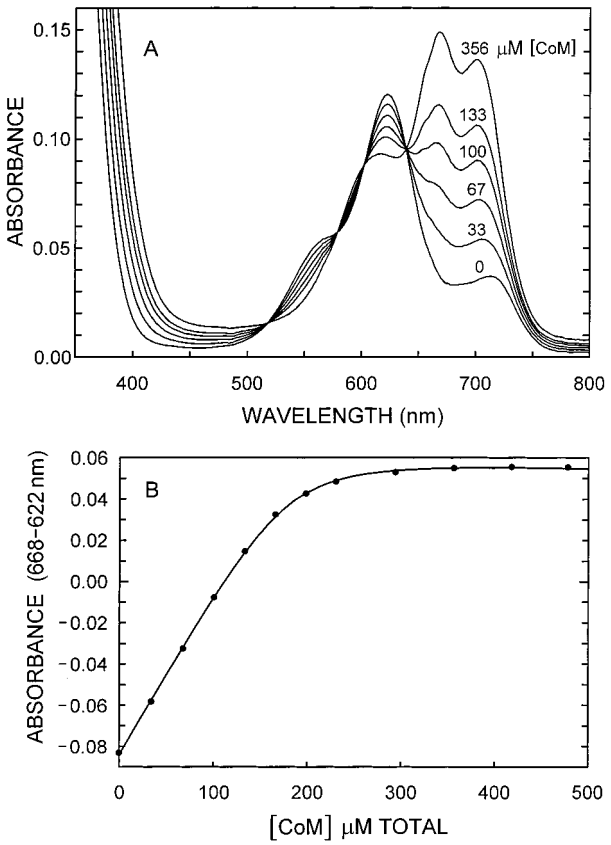


FIGURE 6: Binding of CoM at the metal center of MT2-A. Binding of CoM to MT2-A was detected on the basis of changes in the absorption spectrum of the $Co^{2+}$-substituted enzyme. Panel A: Spectra of a 175 $\mu$M solution of $Co^{2+}$−MT2-A (pH 7.16) obtained before addition of coenzyme M and during titration of the enzyme with CoM at the indicated concentrations. Panel B: Changes in absorbance as a function of total CoM concentration in the titration. The line is drawn from a fit to the quadratic binding equation (Materials and Methods), yielding an apparent dissociation constant $K_d$(obs) = 7.0 $\mu$M.

of total [CoM], as shown in Figure 6B, and was fitted according to the quadratic binding equation to determine the value of the dissociation constant, $K_d$(obs) = 7.0 $\mu$M.

*Proton-Dependent Thermodynamics of CoM Binding*. At pH values much lower than the p$K_a$ of the substrate, ionization of the substrate in the absence of the enzyme can be ignored,[2] and a simple model for proton dissociation accompanying substrate binding can be given according to eq 5, in which E represents $Co^{2+}$−MT2-A and CoM is

$$E + SH \rightleftharpoons ES + H^+ \qquad (5)$$

indicated by SH. The equilibrium constant $K_{eq}$ for such reaction is related to $K_d$(obs) as follows:

$$K_d(\text{obs}) = \frac{[E][SH]}{[ES]} \qquad K_d(\text{obs}) = \frac{[H^+]}{K_{eq}}$$

To examine whether eq 5 was adequate to describe the process of proton release, titration of cobalt-substituted MT2-A with CoM was performed under different conditions

[2] The validity of this assumption was confirmed by calculations made using a formal expression in which acid dissociation of the substrate is incorporated explicitly. Derivation of the expression is given under Supporting Information.

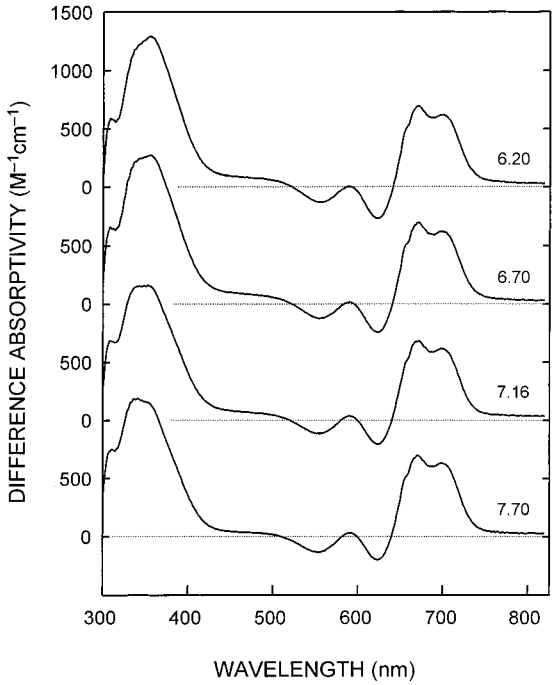


FIGURE 7: Difference spectra produced by reaction of CoM with $Co^{2+}$−MT2-A. Changes in the spectrum of $Co^{2+}$−MT2-A were observed following addition of CoM under different conditions of pH and are plotted as molar absorptivity differences at the values of pH indicated.

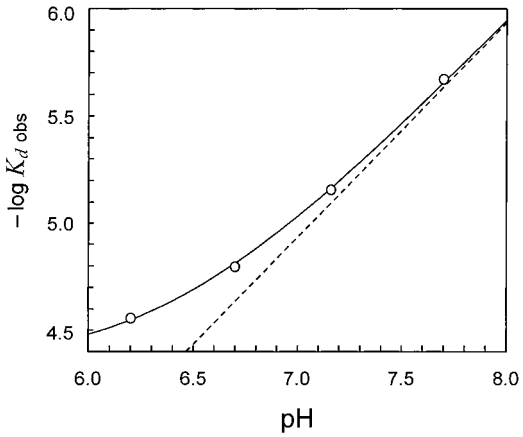


FIGURE 8: pH dependence of CoM binding to MT2-A. Samples of $Co^{2+}$-reconstituted MT2 prepared at different pH values were titrated with CoM, and spectrophotometric data were analyzed to determine values of the apparent dissociation constant, $K_d$(obs). The dashed line represents the model given by eq 5, in which $H^+$ release is concomitant with binding of CoM with a $K_{eq} = 8.8 \times 10^{-3}$. The solid line is drawn from a fit to eq 7, describing binding of CoM as a process separate from net $H^+$ release from a group on the enzyme−CoM complex with an apparent p$K_a$ of 6.4.

of pH, and −log $K_d$(obs) was plotted as a function of pH, as shown in Figure 8. The results indicated an approximate agreement with the predicted linear dependence on pH, but only at the relatively higher values of pH. At lower pH the $K_d$(obs) became increasingly less dependent on proton concentration. A much better representation of the data was given by a two-step (i.e., two-equilibrium) model, as shown in eq 6, in which binding of CoM occurs prior to net proton

$$E + SH \overset{K_1}{\rightleftharpoons} ESH \overset{K_2}{\rightleftharpoons} ES + H^+ \qquad (6)$$

release. In this case, $K_d$(obs), obtained from [E][SH]/[ES +

ESH], is a nonlinear function of pH given by eq 7. The fit

$$K_d(\text{obs}) = \frac{[H^+]}{K_1K_2 + K_1[H^+]} \quad (7)$$

to eq 7 is shown by the solid line in Figure 8 and gave values of $K_1 = 2.2 \times 10^4$ $M^{-1}$ and $K_2 = 4.0 \times 10^{-7}$ M ($pK_a = 6.4$). This analysis assumes that both ESH and ES are spectrophotometrically equivalent, which is supported by the finding that the molar absorptivity of the newly formed 354 nm charge transfer band did not decrease at lower pH and actually increases slightly (10−15%) as the pH decreased over the range of pH 7.7−6.2 (Figure 7). Thus, metal−thiolate coordination appears to be predominant in both ES and ESH complexes, which suggests that direct protonation of the metal−thiolate is not involved and that the proton in the ESH complex resides at a separate site.

## DISCUSSION

We interpret the results of EXAFS analyses and $Co^{2+}$ reconstitution experiments as evidence that coenzyme M binds directly to zinc at the active site of MT2-A. Similar behavior has been observed in cobalamin-independent (MetE) and cobalamin-dependent methionine synthase (MetH) (*16*, *24*) and protein farnesyltransferase (*25*) in the presence of their substrates, suggesting that all four enzymes belong to a family of zinc alkyltransferase enzymes. Herein, we have investigated the affinity of MT2-A for $Zn^{2+}$, explored the nature of ligands in the metal coordination environment, measured the thermodynamics of substrate metal−thiolate bond formation, and characterized factors affecting the activity and metal stoichiometry of MT2-A preparations.

*Activity and Metal Ion Stoichiometry*. The activity of MT2-A was correlated with metal ion content as shown by experiments in which removal of zinc with EDTA resulted in losses of activity and reincorporation of zinc in the presence of a reducing agent resulted in regain of activity (Figures 2 and 3). This agrees with earlier findings of Sauer and Thauer (*10*), who showed that activity of the alternate isozyme MT2-M also correlates with its metal content. In addition, these authors reported activity of MT2-M in the presence of cobalt approximately equal to that observed with the zinc-containing enzyme. Our data show that cobalt-reconstituted MT2-A exhibits markedly higher levels of activity, approximately 16-fold greater than the zinc-containing enzyme. This difference may be due to the intrinsic properties of the two isozymes or may result from differences in the way in which the $Co^{2+}$-containing enzymes were prepared (i.e., anaerobically versus aerobically). Previous studies indicated variability in the metal content of MT2 preparations from 0.4 to 0.9 mol of Zn/mol of MT2 (*8*). Low metal content has been particularly problematic in samples of MT2 purified from *M. barkeri* under aerobic conditions. Although higher levels of zinc were present in recombinant MT2-A purified from *E. coli* grown in the presence of zinc, these preparations also contained less than stoichiometric quantities of zinc. The zinc content and activity could be increased, but only by incubation with $Zn^{2+}$ under reducing conditions. In comparison, oxidation by exposure to a low concentration of $H_2O_2$ yielded a totally inactive form of the enzyme which was completely resistant to metal ion incorporation unless reducing agent was also added, in which case full activity could be restored (Figure 2). These results can be viewed in context with the properties of metallothionein in which the redox state of the sulfur ligands controls the dynamic behavior of the zinc thiolate clusters (*26*). On the basis of results from $Co^{2+}$ titrations and the increase in zinc content observed under reducing conditions, the maximum metal content was found to be 0.90−0.93 mol/mol of MT2-A. We consider that this may in fact represent 1:1 stoichiometry and that deviation from the exact value of 1 could be due to factors affecting determination of the protein concentration. These include the accuracy to which the value of the molar absorptivity coefficient is known and/or the extent to which minor impurities may influence the absorbance of the protein preparations.

Apo MT2-A exhibits a very high affinity for $Zn^{2+}$. At neutral pH the tendency of the apoenzyme to bind $Zn^{2+}$ is even greater than that of EDTA. On the basis of MT2 activity measured in EDTA titrations at pH 7.2, the apparent stability constant for the Zn·MT2-A complex was $10^{13.7}$. This value agrees favorably with the value reported for MT2-M of $\approx 10^{14}$ (*10*). The high affinity explains why apo MT2-A appears to exhibit substantial activity in assay mixtures prepared with very high levels of substrates in the 1−2 mM concentration range (data not shown). Under these conditions metal ion contamination is sufficient to support reactivation occurring in the assay mixture, and addition of even micromolar levels of EDTA to such assays is capable of rapid, total blockage of the apparent activity. In contrast, inactivation of the holoenzyme with EDTA requires tens to hundreds of minutes for equilibrium to be established. This explains a previously reported observation that brief exposure to EDTA followed by gel filtration did not cause a noticeable decrease in the metal content (*8*).

In vivo, MT2-A contains zinc regardless of the exceptionally higher specific activity of the $Co^{2+}$-substituted enzyme. With an interest in the question of why $Zn^{2+}$ was chosen rather than $Co^{2+}$, we carried out measurements of EDTA inhibition also using $Co^{2+}$−MT2-A. The results showed that EDTA is a much stronger inhibitor of $Co^{2+}$−MT2-A than of $Zn^{2+}$−MT2-A, so much so that it was difficult to obtain a precise value for the $K_{eq}$ for EDTA inactivation of the cobalt enzyme analogous to that determined for the zinc enzyme in eq 4. Nevertheless, it was possible to estimate a lower limit for this value of ≈50, which indicates that $Zn^{2+}$ binds to MT2-A with an affinity at least 100 times greater than $Co^{2+}$. The redox-inert nature of $Zn^{2+}$ and its higher abundance relative to cobalt have been considered to explain why zinc enzymes are more widely distributed in nature. However, in methanogens growing in the presence of sulfide it has been estimated that free $Co^{2+}$ should be in excess over free $Zn^{2+}$ (*10*). Furthermore, oxidation to form inactive, substitution-inert $Co^{3+}$ complexes would not be expected under the strictly anaerobic conditions required by these organisms. Rather, our findings suggest that factors relating to the stability of metal ion coordination in MT2 may be responsible for why $Zn^{2+}$, and not $Co^{2+}$, is found in the native protein.

*Metal Ion Coordination Environment*. UV−visible spectroscopy of $Co^{2+}$-containing MT2-A (Figure 5A) indicates tetrahedral geometry of the metal site and, as suggested by high molar absorptivity in the charge transfer band region,

that multiple thiolate coordination is involved. EXAFS analysis of the native zinc-containing protein confirms that the metal center is four-coordinate and contains 2S atoms and 2(N/O) atoms (Table 2). Candidates for providing the two thiolate groups are C241 and C316, whereas one of the N/O atoms is likely to be N from H239, as suggested by results from site-directed mutagenesis and EXAFS data indicating coordination of imidazole. Less information is available regarding the identity of the other N/O ligand. However, our results suggest that the fourth ligand is a group other than histidine and that it is displaced from the metal upon binding of CoM, because EXAFS data indicated that imidazole ligation and coordination number are both maintained upon substrate binding in a 3S + 1N configuration. The changes in number and type of ligands are equivalent to what was reported for MetE and MetH from *E. coli* upon interaction with their substrate homocysteine. However, this pattern differs markedly from that found in rat farnesyltransferase with zinc in a distorted pentacoordinate geometry containing only 1S ligand in the absence, and 2S ligands in the presence of its cysteine-containing peptide substrate (*27*).

*Zinc−Thiolate Intermediate.* Upon binding of CoM the characteristic UV−visible spectrum of $Co^{2+}$−MT2-A exhibits well-defined changes in the region around 600 nm due to d−d transitions as well as in the region between 300 and 400 nm due to $Co^{2+}$−thiolate charge transfer band absorbance (Figures 6A and 7). The magnitude of the absorptivity change arising from CoM metal−thiolate formation of 1150 $M^{-1}$ $cm^{-1}$ did not decline as the pH was decreased from 7.7 to 6.2 (Figure 7). This indicates that the substrate metal−thiolate bond remains intact throughout this range of pH. Direct protonation of the metal−thiolate would greatly decrease the charge transfer band intensity; therefore, it is unlikely that protonation of the metal−thiolate takes place under these conditions. In contrast, the substrate metal−thiolate charge transfer band in farnesyltransferase was strongly attenuated by lowering the pH over a similar range, which was interpreted as evidence for metal−thiolate protonation (*25*). In MT2-A, however, direct protonation of the metal−thiolate would be conceivable only in a range of pH much lower than physiological.

Implicit in the formation of a CoM metal−thiolate bond is the deprotonation of the thiol group of CoM. Nevertheless, a simple model for proton release accompanying the binding of CoM, given by eq 5 (see also eq 5 in ref *10*), does not adequately describe the influence of $[H^+]$ on substrate binding. As the pH was decreased to a value of around pH 6, the apparent dissociation constant, and formation of the metal−thiolate, became substantially less dependent upon $[H^+]$ (Figure 8). The results therefore indicate that thiolate formation occurs in a step separate from release of the proton from the enzyme−substrate complex to the solvent. Although the evidence strongly suggests that protonation takes place at a separate site, not directly on the metal−thiolate, the identity of this site remains to be established. It is possible that a proton becomes associated with the fourth ligand as it is displaced from the metal coordination sphere by CoM, thereby acting as a relay to assist $H^+$ release to bulk solvent. The data indicate an apparent p$K_a$ of 6.4 for the group involved.

*Mechanism of Methyl Group Transfer.* Under in vitro conditions in which methylcobalamin is used as the methyl donor, the overall reaction catalyzed by MT2-A can be considered as the sum of the two partial reactions represented by eqs 8 and 9. The free energy of the second partial reaction,

$$\mathrm{HS{-}CoM + MT2\text{-}A} \overset{K_1}{\rightleftharpoons} \mathrm{[CoM{-}SH{\cdot}MT2\text{-}A]} \overset{K_2}{\rightleftharpoons} \mathrm{CoM{\cdot}MT2\text{-}A + H^+} \quad (8)$$

$$\mathrm{methylcob(III)alamin + CoM{\cdot}MT2\text{-}A} \rightleftharpoons \mathrm{MT2\text{-}A + CH_3{-}S{-}CoM + cob(I)alamin} \quad (9)$$

$$\mathrm{HS{-}CoM + methylcob(III)alamin} \rightleftharpoons \mathrm{CH_3{-}S{-}CoM + cob(I)alamin + H^+} \quad (10)$$

$$\Delta G^{\circ\prime} = -4.90 \text{ kcal/mol } (28)$$

i.e., methyl group transfer (eq 9), can be calculated from the $\Delta G^{\circ\prime}$ of the overall reaction (eq 10) and our data on the thermodynamics of the first reaction of CoM binding and proton release (eq 8). The equilibrium constant for reaction 8 is given by $K_{eq} = K_1K_2$. At pH 7 the value of $K_{eq}' = 8.8 \times 10^4$, which corresponds to $\Delta G^{\circ\prime}$ of −6.7 kcal/mol. The large negative value of −6.7 kcal/mol indicates that metal−thiolate formation in reaction 8 provides a major driving force for the overall reaction. The results also show that methyl group transfer to the metal−thiolate (eq 9) is somewhat unfavorable, with a $\Delta G^{\circ\prime}$ of +1.8 kcal/mol. This may result from the fact that, in contrast to reaction with a free thiolate, direct alkylation of a metal-bound thiolate would be thermodynamically less favorable and potentially unfavorable depending on the alkylating agent used. However, if methyl group transfer actually occurs to a transiently dissociated thiolate, and not to the metal−thiolate directly, as has been suggested in model studies by Wilker and Lippard (*29*), then the nonspontaneous nature of the second partial reaction may be a consequence of the need to carry out the thermodynamically unfavorable dissociation of the metal−thiolate bond. Dissociation of the substrate thiolate would be facilitated by the presence of several other strong ligands at the metal center, and this agrees well with the finding that both cysteine residues and the histidine remain associated in the enzyme−substrate complex. It was found that only a modest increase in the average metal−S bond length occurs upon CoM binding, from 2.30 to 2.33 Å (Table 2); however, it is difficult to interpret from the average whether the strength of the CoM metal−thiolate interaction is comparable to that of the exchangeable fourth ligand. It may be envisioned that the strength of the bond between the fourth ligand and the metal would be intermediate between that of CoM ligation and that of the more weakly coordinating thioether group of the product methyl-CoM; this would favor the displacement of the fourth ligand by the substrate and allow for its subsequent religation in expulsion of the product. It will be most interesting to correlate the biochemical and spectroscopic properties of MT2-A described herein with a detailed structure from crystallographic studies.

*CoM Methylation in Other Steps in Methanogenesis.* Our results indicate that capture of CoM by binding and coordination at the active site of MT2 is the most exergonic step yet described in the pathways leading from methanol or methylated amine substrates to methyl-CoM. This suggests that methanogens might take advantage of the energy

available from this type of reaction as well in other processes involving CoM binding and methylation. One such reaction, involved in growth on acetate or on $CO_2 + H_2$, is methyl group transfer from the folate analogue $N^5$-methyltetrahydrosarcinapterin (or $N^5$-methyltetrahydromethanopterin in some species) to CoM catalyzed by Mtr, the membrane-associated, corrinoid-containing multienzyme complex. This reaction occurs with a $\Delta G^{\circ\prime}$ of $-7.2$ kcal/mol, and energy is conserved by coupling methyl group transfer to the transmembrane extrusion of sodium ions (for a recent review, see ref *30*). Although full details of the coupling are not yet available, it is reasonable to consider that CoM binding might also provide a major part of the driving force for ion translocation in this system.

## SUPPORTING INFORMATION AVAILABLE

Derivation of formal expressions for the pH dependence of the $K_d$(obs) incorporating acid dissociation of the substrate for both models described in the text. This material is available free of charge via the Internet at http://pubs.acs.org.

## REFERENCES


1. Burke, S. A., and Krzycki, J. A. (1995) *J. Bacteriol. 177*, 4410−4416.
2. Sauer, K., Harms, U., and Thauer, R. K. (1997) *Eur. J. Biochem. 243*, 670−677.
3. Ferguson, D. J., Jr., and Krzycki, J. A. (1997) *J. Bacteriol. 179*, 846−852.
4. Tallant, T. C., and Krzycki, J. A. (1997) *J. Bacteriol. 179*, 6902−6911.
5. Ferguson, D. J., Jr., Gorlatova, N., Grahame, D. A., and Krzycki, J. A. (2000) *J. Biol. Chem. 275*, 29053−29060.
6. Grahame, D. A. (1989) *J. Biol. Chem. 264*, 12890−12894.
7. Ferguson, D. J., Jr., Krzycki, J. A., and Grahame, D. A. (1996) *J. Biol. Chem. 271*, 5189−5194.
8. LeClerc, G. M., and Grahame, D. A. (1996) *J. Biol. Chem. 271*, 18725−18731.
9. Myers, L. C., Terranova, M. P., Ferentz, A. E., Wagner, G., and Verdine, G. L. (1993) *Science 261*, 1164−1167.
10. Sauer, K., and Thauer, R. K. (2000) *Eur. J. Biochem. 267*, 2498−2504.
11. Matthews, R. G., and Goulding, C. W. (1997) *Curr. Opin. Chem. Biol. 1*, 332−339.
12. Hightower, K. E., and Fierke, C. A. (1999) *Curr. Opin. Chem. Biol. 3*, 176−181.
13. Johnson, A. W., Mervyn, L., Shaw, N., and Smith, E. L. (1963) *J. Chem. Soc.*, 4146−4156.
14. Perkins, S. J. (1986) *Eur. J. Biochem. 157*, 169−180.
15. Kunkel T. A. (1985) *Proc. Natl. Acad. Sci. U.S.A. 82*, 488−482.
16. González, J. C., Peariso, K., Penner-Hahn, J. E., and Matthews, R. G. (1996) *Biochemistry 35*, 12228−12234.
17. Peariso, K., Goulding, C. W., Huang, S., Matthews, R. G., and Penner-Hahn, J. E. (1998) *J. Am. Chem. Soc. 120*, 8410−8416.
18. Clark-Baldwin, K., Tierney, D. L., Govindaswamy, N., Gruff, E. S., Kim, C., Berg, J., Koch, S. A., and Penner-Hahn, J. E. (1998) *J. Am. Chem. Soc. 120*, 8401−8409.
19. Rehr, J. J., deLeon, J. M., Zabinsky, S. I., and Albers, R. C. (1991) *J. Am. Chem. Soc. 113*, 5135−5140.
20. Rehr, J. J., Albers, R. C., and Zabinsky, S. I. (1992) *Phys. Rev. Lett. 69*, 3397−3400.
21. Segel, I. H. (1975) *Enzyme Kinetics*, John Wiley and Sons, New York.
22. Dawson, R. M. C., Elliot, D. C., Elliot, W. H., and Jones, K. M. (1986) Stability constants for metal complexes, in *Data for Biochemical Research*, 3rd ed., Chapter 17, Oxford University Press, New York.
23. Grahame, D. A., Khangulov, S., and DeMoll, E. (1996) *Biochemistry 35*, 593−600.
24. Peariso, K., Zhou, Z. S., Smith, A. E., Matthews, R. G., and Penner-Hahn, J. E. (2001) *Biochemistry 40*, 987−993.
25. Hightower, K. E., Huang, C.-C., Casey, P. J., and Fierke, C. A. (1998) *Biochemistry 37*, 15555−15562.
26. Maret, W., and Vallee, B. L. (1998) *Proc. Natl. Acad. Sci. U.S.A. 95*, 3478−3482.
27. Park, H.-W., Boduluri, S. R., Moomaw, J. F., Casey, P. J., and Beese, L. S. (1997) *Science 275*, 1800−1804.
28. Sauer, K., and Thauer, R. K. (1997) *Eur. J. Biochem. 249*, 280−285.
29. Wilker, J. J., and Lippard, S. J. (1997) *Inorg. Chem. 36*, 969−978.
30. Gottschalk, G., and Thauer, R. K. (2001) *Biochim. Biophys. Acta 1505*, 28−36.


BI0112917